

## Analysis of the morphology and properties of PAN/Bi<sub>2</sub>O<sub>3</sub> composite nanomaterials produced by electrospaying method

T. Tański <sup>a,b</sup>, W. Matysiak <sup>a,\*</sup>, L. Markovičová <sup>c</sup>, N. Florek-Szotowicz <sup>a</sup>,  
P. Snopiński <sup>a</sup>, Ł. Krzemiński <sup>a</sup>, M. Wiśniowski <sup>a</sup>

<sup>a</sup> Department of Materials Processing Technology, Management and Technology in Materials, Institute of Engineering Materials and Biomaterials, Silesian University of Technology, Gliwice, Poland

<sup>b</sup> Center of Nanotechnology, Silesian University of Technology, Gliwice, Poland

<sup>c</sup> Department of Materials Engineering, Mechanical Engineering, University of Žilina, Žilina, Slovak Republic

\* Corresponding e-mail address: wiktormatysiak@polsl.pl

### ABSTRACT

**Purpose:** The aim of the study was the preparation of the composite nanofibers with the polymer matrix reinforced by the reinforcement phase in the form of Bi<sub>2</sub>O<sub>3</sub> ceramic nanoparticles using the electrospinning method from the 10% PAN/DMF solutions with the mass concentration of Bi<sub>2</sub>O<sub>3</sub> nanoparticles of the order of 5 and 10%, and the investigate their morphology and physical properties as a function of the mass concentration of the reinforcing phase and the applied process parameters.

**Design/methodology/approach:** In order to analyze the structure of the used Bi<sub>2</sub>O<sub>3</sub> nanoparticles were used high-resolution transmission electron microscope (TEM) and X-ray diffraction analysis (XRD). To examine the morphology and chemical composition of the resulting of materials was carried out using a scanning electron microscope (SEM) with energy dispersive spectrometer (EDS). In order to analyze the physical properties of obtained composite materials was made the UV-VIS spectroscopy study, which are then used to determine the band structure of the obtained nanocomposite materials and to determine the effect of mass concentration of the reinforcing phase on the value of the energy band gap.

**Findings:** The influence of parameters of the electrospinning process on morphology of the composite materials and influence of mass concentration of reinforcing phase on electrical structure obtained materials were determined.

**Practical implications:** Analysis of the electrical properties resulting composite material showed that the PAN composite material reinforced ceramic Bi<sub>2</sub>O<sub>3</sub> nanoparticles is a potentially attractive dielectric material which may be used in the field of optoelectronics.

**Originality/value:** The Bi<sub>2</sub>O<sub>3</sub> particles, due to their energy structure and the photocatalytic properties applied as the strengthening phase for polymers fibers and particles are attractive alternative for composite materials from PAN/TiO<sub>2</sub> used as the photocatalytic and dielectric materials.

**Keywords:** Electrospinning/electrospraying method; Polymer composite materials; Polyacrylonitrile; Bi<sub>2</sub>O<sub>3</sub> nanoparticles, energy band gap

**Reference to this paper should be given in the following way:**

T. Tański, W. Matysiak, L. Markovičová, N. Florek-Szotowicz, P. Snopiński, Ł. Krzemiński, M. Wiśniowski, Analysis of the morphology and properties of PAN/Bi<sub>2</sub>O<sub>3</sub> composite nanomaterials produced by electrospraying method, Journal of Achievements in Materials and Manufacturing Engineering 73/2 (2015) 176-184.

## PROPERTIES

### 1. Introduction

The electrospinning process consists in subjecting a stream of dissolved polymer to electric field, whereby under the influence of electrostatic forces a stream of polymer rotates along the field lines reducing its diameter. Controlled selection of the process parameters and used mixture allows to obtain micro/nanofibers or micro/nanoparticles [1-4].

During the outflow of polymer stream from the nozzle, several zones can be distinguished. The first of them is a solution of polymer in a nozzle. At this stage microparticles of polymer preliminary oriented in the outflow direction. In the second zone polymer leaves the nozzle forming a shape of Taylor's cone. The degree of stream orientation depends on the flow rate of the solution and length of the nozzle. By the action of electrostatic field, on the surface of Taylor's cone accumulates an electric charge and when the charge density at the tip of cone exceeds (in terms of energy) the value of the surface tension of solution, cone takes the form of straightforward stream of solution. The stream is subjected to the electric field action, which result in obtaining bipolar electric layer in which one type of electric charges are directed inside and the second are directed outside of the stream of the polymer. In this way at the surface of the stream an electric potential is produced which interacts with the external field causing strong tension of the polymer stream. Along with increasing length of the stream the value of the electric charge increases, that in some moment, reaches a critical value and result in flow of the stream. In the last stage of the process the deposition of produced material on the surface of the collector and evaporation of the solvent occurs [4,5].

PAN nanofibers, produced by electrospinning process have found the application in many areas of life. Because of its porosity of the order of 72%, are used inter alia, as the membranes in the new generation of lithium-ion batteries and also in solar and fuel cells [6-9]. Studies have shown that nanofibres from polyacrylonitrile are very good support for ceramic nanoparticles, which increases its application field [10-14]. Particularly noteworthy are the PAN nanofibers reinforced by Bi<sub>2</sub>O<sub>3</sub> nanoparticles. These particles, due to their energy

structure [15] and the photocatalytic properties [16] applied as the strengthening phase for polymers fibers are attractive alternative for composite mats from PAN/TiO<sub>2</sub> used as the photocatalytic materials.

### 2. Materials and work methodology

For preparation of the spinning solution polyacrylonitrile polymer was used (purity 99%, Mw=150 000 g/mol). As the solvent N,N-dimethylformamide was used (99.8% purity). The reinforcing phase used in current study was Bi<sub>2</sub>O<sub>3</sub> nanoparticles (purity 99%, size of particles 35-230 nm). The final product was solution of DMF/PAN/nanoparticles Bi<sub>2</sub>O<sub>3</sub> with weight concentration of the polymer of 5%, 10% and 5 and 10 % of weight concentration of nanoparticles. In order to break agglomerates of reinforcing phase, measured amount of nanoparticles was added to N,N dimethylformamide and these solutions were subjected to sonication process for 0,5 h. After the sonication process, to the solution, a measured amount of the polymer was added and this solution was subjected to magnetic stirring for a time of 24 hours at room temperature. The polymer nanofibres were obtained using the electrospinning method using FLOW-Nanotechnology Solutions Electrospinner 2.2.0-500 system. Process parameters are listed in Table 1.

To investigate the chemical composition of reinforcing phase, X-ray diffraction phase analysis was performed using X'Pert Pro Analytical diffractometer with Cu anode ( $\lambda K\alpha = 0,17909$  nm). The X-ray tube was supplied with the current I= 40 mA under a voltage of U=40 kV. Diffraction examinations were performed within the range of angles  $2\theta$  from 20° to 120°. The measurement step was 0.026° in length whilst the pulse counting time was 30s.

To solve obtained diffraction patterns, dedicated database of ICSD files was used. In order to present the morphology of reinforcing Bi<sub>2</sub>O<sub>3</sub> nanoparticles, high resolution transmission electron microscope Titan 80-300 supplied by FEI with HAADF detector.

The produced composite material was subjected to quantitative and qualitative analysis using EDX

microanalysis and surface topography imaging using Scanning Electron Microscope with X-Ray spectrometer Trident XM4 supplied by EDAX. Basing on the obtained SEM images at the magnification 50000, measurement of the diameter of nanofibers and nanoparticles was prepared, using DigitalMicrograph application, followed by determination of the average value and the chemical composition basing on the spectrum analysis. Absorbance measurements of the obtained material, from which the value of band gap was calculated, were performed using UV/VIS Evolution 220 spectrometer supplied by Thermo-Scientific. During the measurement light beam having a wave length in the range of 190-1100nm fell perpendicularly to the sample.

### 3. Results and discussion

#### 3.1. Chemical analysis of the $\text{Bi}_2\text{O}_3$ nanoparticles

X-ray analysis of the investigated particles unequivocally shows, that obtained diffraction lines on the diffraction pattern correspond to the tetragonal crystal structure  $\beta\text{-Bi}_2\text{O}_3$  with a space group P-4 2 1 according to the JCPDS-ICDD database (card 98-005-2732). The morphology analysis prepared basing on the TEM images shows that particles have spherical shape and their diameter is in the range of 35-230 nm (Fig. 1).

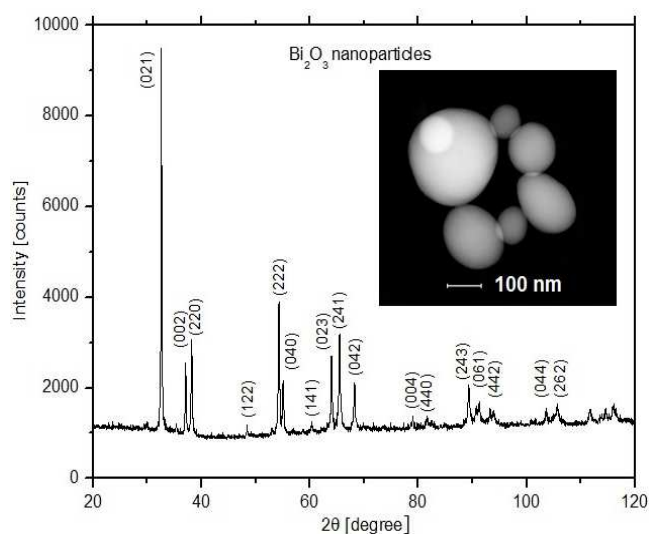


Fig. 1. The XRD spectrum of investigated  $\text{Bi}_2\text{O}_3$  nanoparticles and TEM image showing their morphology

#### 3.2. Analysis of the morphology of the obtained materials

In order to prepare the morphology analysis of the of the obtained composite materials, a surface topography imaging utilizing Scanning Electron Microscope was used. In case of all four obtained samples that were made by application of process parameters listed in Table 1, results of the experiment were composite particles  $\text{PAN}/\text{Bi}_2\text{O}_3$ . For samples that were made from solutions containing 5% of nanoparticles of bismuthum oxide, nanoparticles were obtained, but when the concentration of ceramic particles was 2 times greater, result of the electrospinning process were microparticles. An analysis of the morphology and structure of sample 1 obtained from 10% solution of  $\text{PAN}/\text{DMF}$  (5% weight concentration), by appliance solution flow rate of 0.35 ml/h, shows that, as a result of applied process parameters, spherical and lamellar particles were obtained (pollen particles), that presents figure 2. Fiftyfold measurement of the diameter of obtained nanoparticles of  $\text{PAN}/\text{Bi}_2\text{O}_3$  shows that, value of the measured diameters are within the range of 200 – 1800 nm, wherein, the most frequently occurring values of the diameters, were within the range of 400 to 600 nm, which represents 28% of all the measured diameter values for this sample (Fig. 2 - histogram).

Structure analysis of the obtained composite materials of  $\text{PAN}$  reinforced by  $\text{Bi}_2\text{O}_3$  particles with 5% mass concentration (sample 2), using twice greater spinning solution flow rate (0.7 ml/h), showed, that for this sample also nanoparticles of  $\text{PAN}/\text{Bi}_2\text{O}_3$  were obtained (Fig. 2). The analysis of the morphology on the basis of SEM images showed that nanoparticles are characterized by spherical and lamellar morphology whereas the size of measured particles were within the range of ~ less than 200 nm to 1400 nm. The largest group, containing 32% of the obtained particles in sample 2, were nanoparticles that had diameters within the range of 400 to 600 nm. Quantitative chemical composition analysis prepared on the basis of EDX spectrum for sample obtained from 10% solution of  $\text{PAN}/\text{DMF}$  containing  $\text{Bi}_2\text{O}_3$  nanoparticles with 5% mass concentration, confirmed the presence of obtained polymer nanoparticles (Fig. 6-sample 2).

Application of the spinning solution of  $\text{PAN}/\text{DMF}$  with twice higher mass concentration (10%) of bismuth oxide nanoparticles, comparing to the solution used to obtain sample 1 and 2 had contributed to obtaining microparticles with lamellar morphology (Fig. 3). In case of the sample 3, obtained from solution with 10% concentration of  $\text{Bi}_2\text{O}_3$  nanoparticles and using lower solution flow rate of 0.35 ml/h, an morphology analysis showed that composite particles had diameters within the range of 400 nm to 2 mm (Fig. 4).

Table 1.  
The parameters of the samples production process

The process parameters	Sample 1	Sample 2	Sample 3	Sample 4
The mass concentration of PAN	10%	10%	10%	10%
The mass concentration of $\text{Bi}_2\text{O}_3$	5%	5%	10%	10%
The solution flow rate, ml/h	0.35 ml/h	0.7 ml/h	0.35 ml/h	0.7 ml/h
The distance between the electrodes, cm	12.5 cm	12.5 cm	12.5 cm	12.5 cm
The potential difference between the electrodes, kV	15kV	15kV	15kV	15kV

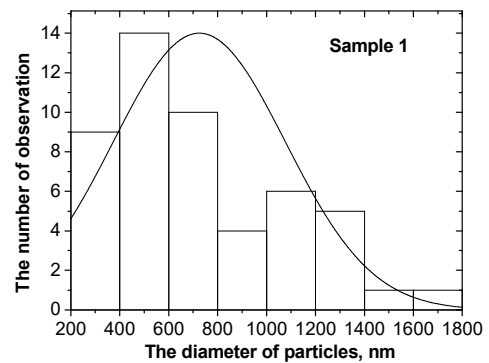
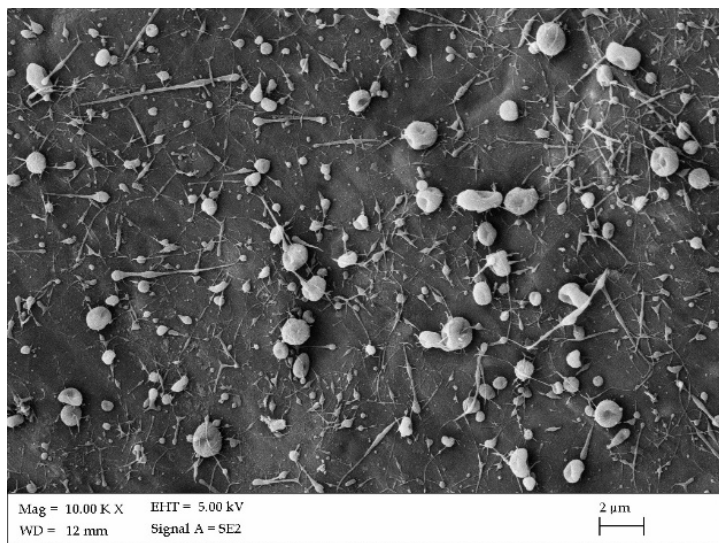


Fig. 2. The SEM image of morphology of obtained PAN/ $\text{Bi}_2\text{O}_3$  particle, and a histogram showing the distribution of measured diameters - sample 1

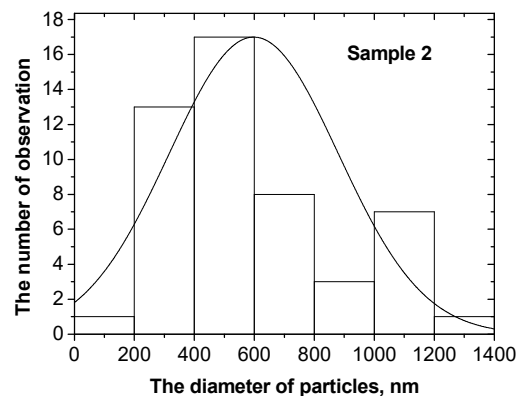
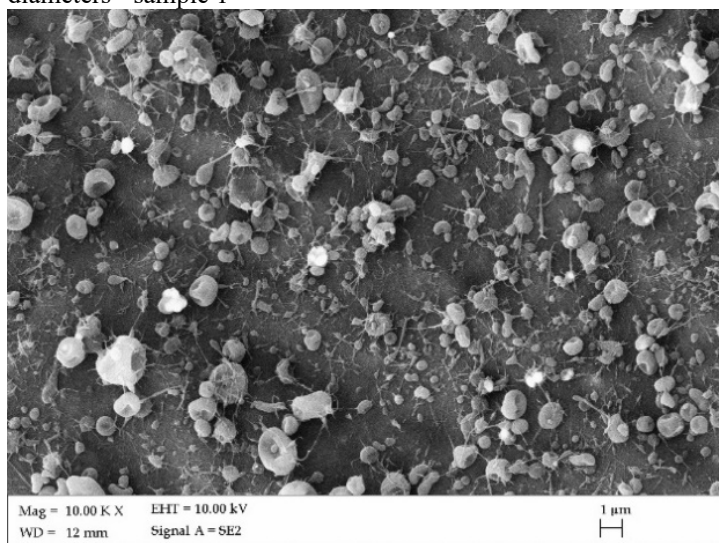


Fig. 3. The SEM image of morphology of obtained PAN/ $\text{Bi}_2\text{O}_3$  particle, and a histogram showing the distribution of measured diameters - sample 2

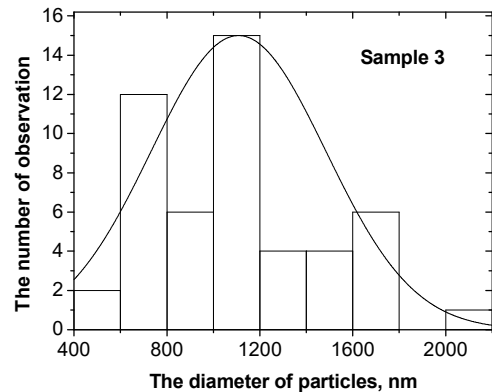
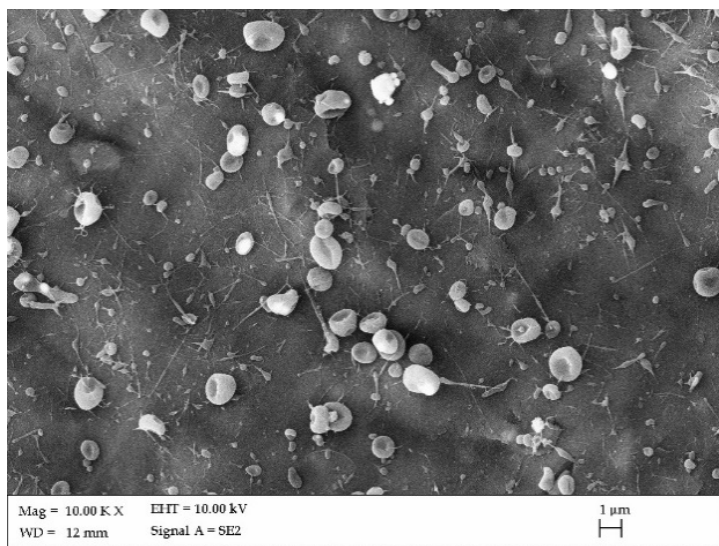


Fig. 4. The SEM image of morphology of obtained PAN/Bi<sub>2</sub>O<sub>3</sub> particle, and a histogram showing the distribution of measured diameters - sample 3

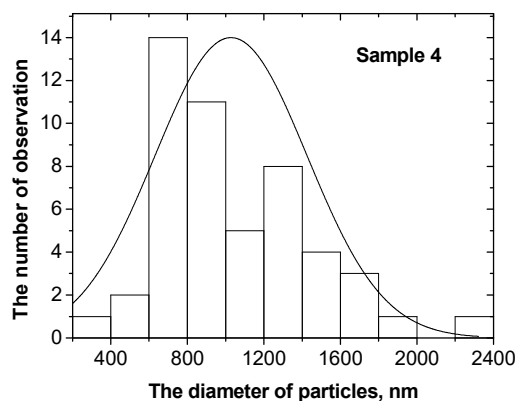
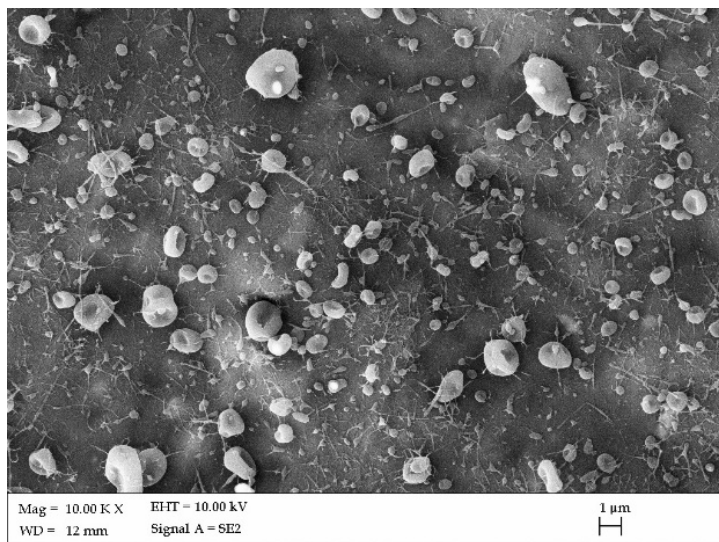


Fig. 5. The SEM image of morphology of obtained PAN/Bi<sub>2</sub>O<sub>3</sub> particle, and a histogram showing the distribution of measured diameters - sample 4

The most common group particles constituting approx. 30% of all particles of the sample 3 are composite particles of PAN / 10% Bi<sub>2</sub>O<sub>3</sub> with diameters within the range of 1 to 1.2 mm (Fig. 4 - histogram). Application of twice greater spinning solution flow rate of 0.7 ml/h for sample containing 10% of Bi<sub>2</sub>O<sub>3</sub> nanoparticles (sample 4) contributes to obtaining microparticles with lamellar morphology as it was in case of sample 3 (Fig. 5). Values of measured diameters for sample 4 varies within the range of

200 nm – 2.2 mm. The most common group of particles are these in the range of 600-800 nm (Fig. 5 – histogram). An EDS microanalysis of sample 4 showed that, similarly as in the case of sample 3, there is the presence of Bi<sub>2</sub>O<sub>3</sub> particles in the polymer microparticles.

Table 2 presents the results of the diameter measurements of obtained composite particles. Both in the case of used PAN/DMF solution containing 5 % and 10 % of Bi<sub>2</sub>O<sub>3</sub> nanoparticles, change in solution flow rate from

0.35 to 0.7 ml contributes to decrease in the diameter of obtained composite nanoparticles. For samples 1 and 2 the decrease in diameter was about 126 nm. For samples 2 and 3, increased solution flow rate result in decrease in particles diameter of about 83 nm. An important factor appear also the concentration of reinforcing particles in spinning

solution. Application of 10% concentration of  $\text{Bi}_2\text{O}_3$  nanoparticles using same parameters of electrospinning process result in an increase of diameter of obtained composite materials. For this materials (sample 3 and 4) the average value of increase of diameters was 800 nm.

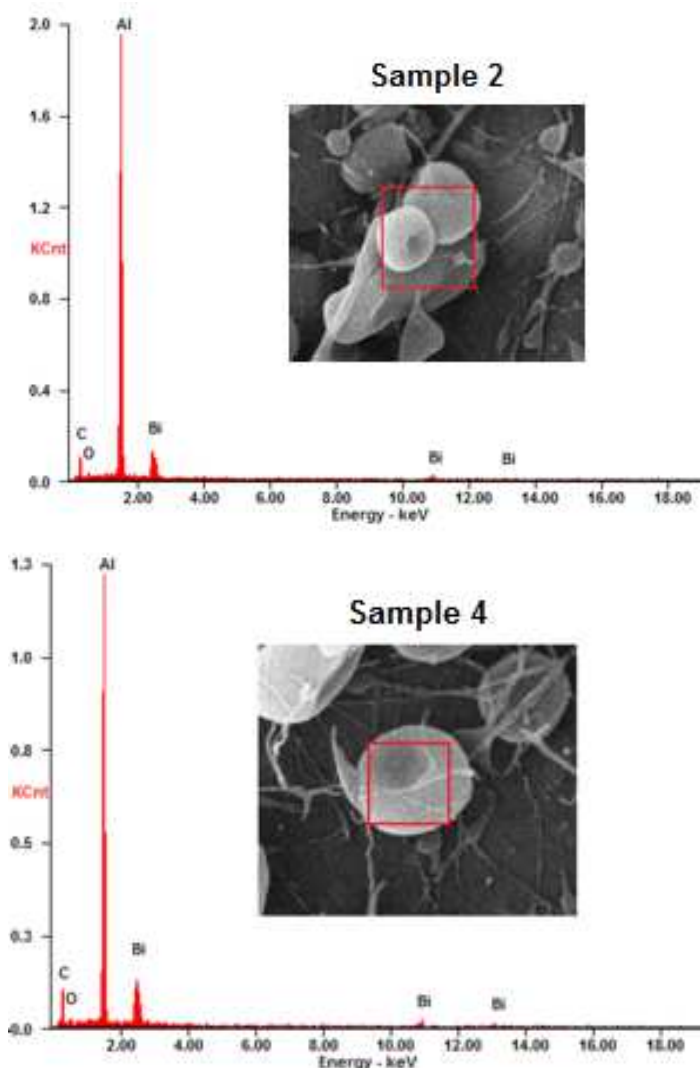


Fig. 6. EDX spectra of obtained composite particles for Sample 2 (the concentration of  $\text{Bi}_2\text{O}_3$  nanoparticles 5%) and sample 4 (concentration of  $\text{Bi}_2\text{O}_3$  nanoparticles 10%)

### 3.3. Analysis of the electrical properties of the obtained materials

In order to determine the electrical band structure of obtained composite materials was used the UV-Vis study. For

each of the prepared sample was measured the absorbance ABS in function of wavelength of electromagnetic radiation  $\lambda$ . Next, using the equation linking absorbance ABS and transmittance T:

$$ABS = -\log(T) \quad (1)$$

Table 2.

The average value of the particles diameters of the obtained composite materials

Number of sample	Sample 1	Sample 2	Sample 3	Sample 4
The average value of the particles diameter, nm	725	598	1108	1025

Table 3.

The value of the energy band gap of the obtained composite materials

Number of sample	Sample 1	Sample 2	Sample 3	Sample 4
The energy band gap, eV	$3.79 \pm 0.25$	$3.77 \pm 0.22$	$3.82 \pm 0.23$	$3.84 \pm 0.25$

Given the above equation, and also assuming that the phenomenon of reflectivity occurring at the air - the sample was negligible, equation describing the relationship between the absorption coefficient  $\alpha$  of the test material and wavelength  $\lambda$  of the incident radiation on the sample:

$$\alpha h\nu = A(h\nu - E_g)^{1/2} \quad (2)$$

where  $h$  is Planck's constant,  $A$  is a constant dependent on the type of electronic transitions,  $\nu$  is the frequency of the radiation, takes the following form:

$$\left[ h\nu \ln \left( \frac{1}{10^{-ABS}} \right) \right]^2 = B(h\nu - E_g) \quad (3)$$

Then, plotted graphs of depending of  $\left[ h\nu \ln \left( \frac{1}{10^{-ABS}} \right) \right]^2$  as a function of the quantum energy radiation for all the samples prepared and adjusted linear functions for the straight sections of the graph with the largest coefficients directional line (Fig. 7). Zero of linear function, determined by calculating the absolute value of the ratio of words available to the direction numbers match-fit line width of the energy gap of the tested composite materials. Table 3 shows the results of the width of the energy band gap of the prepared samples.

An analysis of the obtained results of band gap measurements, for composite material showed that with increasing mass concentration of reinforcing phase, an increased in value of band gap is observed.

For nanoparticles containing PAN/5%  $\text{Bi}_2\text{O}_3$  nanoparticles the value of band gap was 3.78 eV. An increased of mass concentration of ceramic nanoparticles to 10% result in obtaining composite microparticles with greater value of energy gap of 3.83 eV. An increased of band gap is accompanied by greater concentration of ceramic

nanoparticles which is caused by the nature of this particles [17].

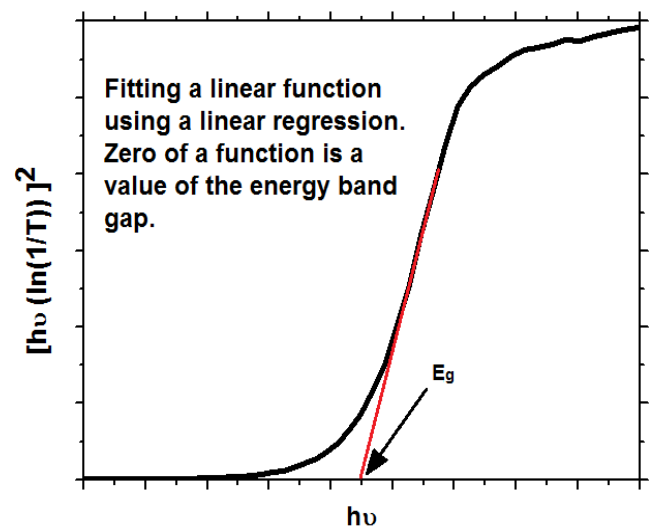


Fig. 7. Method of determining the width of the energy gap on the basis of spectrophotometric UV-Vis

Application of dielectric nanoparticles contributed to change in the value of band gap for obtained composite material in comparison to pure PAN polymer, which value of band gap is 2.23 eV [18].

In addition, the energy band gap of obtained composite materials is also characterized by a much higher value in relation to the pure nanoparticles  $\beta\text{-Bi}_2\text{O}_3$ , for which the average value of the energy gap determined experimentally amounts to approx. 2.7 eV [19] and for commonly used in electronics thin layers of  $\text{TiO}_2$  [20], whose energy gap was determined on the basis of UV-Vis spectra by the authors is  $2.93 \pm 0.08$  eV. The analysis of the energy structure of PAN/ $\text{Bi}_2\text{O}_3$  composite nanomaterials showed a good

dielectric properties of such materials, thus making them potentially attractive dielectric materials for applications in the electronics industry.

#### 4. Conclusions

By application of electrospinning method, from 10% solution of PAN/DMF containing mass concentration of ceramic nanoparticles of  $\text{Bi}_2\text{O}_3$  successively 5 and 10%, a composite nanoparticles were obtained. An surface topography analysis, prepared using Scanning Electron Microscope revealed that for solution containing 5% of reinforcing phase, obtained nanoparticles were characterized by spherical and lamellar morphology and the size of diameter was 662 nm. Application of solution with greater concentration of nanoparticles (10%), result in obtaining lamellar composite particles with size of diameters of 1067 nm. Analysis of the electrical properties (electrical band structure) of the materials obtained composite was made on the basis of spectra of UV-Vis showed that the composite material PAN reinforced ceramic nanoparticles  $\text{Bi}_2\text{O}_3$  is a potentially attractive dielectric material which may be used in the field of optoelectronics.

#### Acknowledgements

Project was funded by the National Science Centre, Paland based on the decision number 2014/15/B/ST8/04767

#### References

- [1] A. Frenot, I.S. Chronakis, Polymer nanofibers assembled by electrospinning, *Current Opinion in Colloid and Interface Science* 8 (2003) 64-75.
- [2] Q.F. Wei, F.L. Huang, Surface functionalisation of polymer nanofibres by sputter coating of titanium dioxide, *Applied Surface Science* 252 (2006) 7874-7877.
- [3] A. Aytimur, S. Koçyi, Fabrication and characterization of bismuth oxide/holmia nanofibers and nanoceramics, *Current Applied Physics* 13 (2013) 581-586.
- [4] M.P. Prabhakaran, M. Zamani, B. Felice, S. Ramakrishna, Electrospinning technique for the fabrication of metronidazole contained PLGA particles and their release profile, *Materials Science and Engineering C* 56 (2015) 66-73.
- [5] F.K. Ko, A. Goudarzi, L. Lin, Y. Li, J.F. Kadla, 9-lignin-based composite carbon nanofibers, *Lignin in Polymer Composites* (2016) 167-194.
- [6] S. Agarwala, A. Greinera, J.H. Wendorff, Functional materials by electrospinning of polymers *Progress in Polymer Science* 38 (2013) 963-991.
- [7] M. Naraghi, S.N. Arshad, I. Chasiotis, Molecular orientation and mechanical size effects in electrospun polyacrylonitrile nanofibers, *Polymer* 52 (2011) 1612-1618.
- [8] R. Luoh, H. Thomas Hahn, Electrospun nanocomposite fiber mats as gas sensors, *Composites Science and Technology* 66 (2006) 2436-2441.
- [9] T. Choa, M. Tanakab, H. Onishi, Battery performances and thermal stability of polyacrylonitrile nano-fiber-based nonwoven separators for Li-ion battery, *Journal of Power Sources* 181 (2008) 155-160.
- [10] C. Praharn, W. Klinsukhon, N. Roungpaisan, Electrospinning of PAN/DMF/H<sub>2</sub>O containing TiO<sub>2</sub> and photocatalytic activity of their webs, *Materials Letters* 65 (2011) 2498-2501.
- [11] L. Ji, Z. Lin, A. J. Medford, X. Zhang, Porous carbon nanofibers from electrospun polyacrylonitrile/ SiO<sub>2</sub> composites as an energy storage material, *Carbon* 47 (2009) 3346-3354.
- [12] J.S. Im, M.I. Kim, Y.S. Lee, Preparation of PAN-based electrospun nanofiber webs containing TiO<sub>2</sub> for photocatalytic degradation, *Materials Letters* 62 (2008) 3652-3655.
- [13] S. Fang, W. Wang, X. Yu, H. Xu, Y. Zhong, Preparation of ZnO:(Al, La)/ polyacrylonitrile (PAN) nonwovens with low infrared emissivity via electrospinning, *Materials Letters* 143 (2015) 120-123.
- [14] S. Dadvar, H. Tavanai, M. Morshed, Fabrication of Nanocomposite PAN Nanofibers Containing MgO and Al<sub>2</sub>O<sub>3</sub> Nanoparticles, *Polymer Science* 56 (2014) 358-365.
- [15] M. Jalalah, M. Faisal, H. Bouzid, J. Park, S.A. Al-Sayari, A.A. Ismail, Comparative study on photocatalytic performances of crystalline  $\alpha$ - and  $\beta$ -Bi<sub>2</sub>O<sub>3</sub> nanoparticles under visible light, *Journal of Industrial and Engineering Chemistry* 30 (2015) 183-189.
- [16] H. Oudghiri-Hassani, S. Rakass, F.T. Al Wadaani, K.J. Al-ghamdi, A. Omer, M. Messali, M. Abboudi, Synthesis, characterization and photocatalytic activity of  $\alpha$ -Bi<sub>2</sub>O<sub>3</sub> nanoparticles, *Journal of Taibah University for Science* 9/4 (2015) 508-512.
- [17] E.T. Salim, Y. Al-Douri, M.S. Al Wazny, M.A. Fakhri, Optical properties of Cauliflower-like Bi<sub>2</sub>O<sub>3</sub>



- nanostructures by reactive pulsed laser deposition (PLD) technique, *Solar Energy* 107 (2014) 523-529.
- [18] A. Koganemaru, Y. Bin, Y. Agari, M. Matsuo, Composites of polyacrylonitrile and multiwalled carbon nanotubes prepared by gelation/crystallization from solution, *Advanced Functional Materials* 14 (2004) 842-850
- [19] J. Zhang, W. Dang, X. Yan, M. Li, Z. Ao, Doping indium in  $\beta$ - $\text{Bi}_2\text{O}_3$  to tune the electronic structure and improve the photocatalytic activities: first-principles calculations and experimental investigation, *Physical Chemistry Chemical Physics* 16 (2014) 23476-2348.
- [20] A.F. Khan, M. Mehmood, S.K. Durrani, M.L. Ali, N.A. Rahim, Structural and optoelectronic properties of nanostructured  $\text{TiO}_2$  thin films with annealing, *Materials Science in Semiconductor Processing* 29 (2015) 161-169.